



# Stress concentration coefficients of optimized cope-hole welded detail

Ping Liao<sup>1</sup> · Renda Zhao<sup>1</sup> · Xing Wei<sup>1</sup> · Yi Jia<sup>1</sup> · Lingzhi Cui<sup>1</sup> · Yongbao Wang<sup>1</sup>

Received: 27 April 2017/Revised: 5 September 2017/Accepted: 6 September 2017/Published online: 18 September 2017  
© The Author(s) 2017. This article is an open access publication

**Abstract** The fatigue performance of optimized welded detail has been investigated by fatigue experiments of three welded specimens under different loadings. In addition, local finite element models of this welded detail were established using finite element software ANSYS. The influences of different factors such as plate thickness, plate gap and initial geometric imperfections on the stress concentration coefficient (SCC) were discussed. The experimental results indicate that the fatigue life of three specimens for this welded detail is 736,000, 1,044,200 and 1,920,300 times, respectively. The web thickness, the filler plate thickness and the initial geometric imperfection have relatively less effect on the SCCs of this welded detail. However, cope-hole radius is influential on the SCCs of the web and the weld. The SCC of weld is significantly affected by the weld size and plate gap, but the SCCs of other parts of the welded detail are hardly affected by the plate gap.

**Keywords** Steel bridge · Optimized welded detail · Fatigue performance · Fatigue experiment · Stress concentration coefficient (SCC) · Cope hole · Plate thickness · Initial geometric imperfection

## 1 Introduction

Due to many advantages such as light weight, large span capacity and beautiful shape, steel bridges have been widely used in bridge construction. Some welded structure

details about cope holes to avoid weld cross appear during the design and construction stage. However, these details are always subjected to repeated cyclic loads in practice, and fatigue cracks may develop and result in fatigue damage or failure. These fatigue cracks are always initiated at the weld toe of the flange for these details, where high local stress concentration is induced by the structural discontinuity or weld defections. Thus, fatigue assessment and analysis of these welded details are necessary for bridges under repeated cyclic loads [1].

Chiew et al. [2] conducted fatigue tests to measure and analyze fatigue strength and local stresses for cope-hole details existing in I-section beams bent in-planes. The research results indicated that the fatigue strength of cope-hole details was extremely low because of the local stress around the cope holes. Park et al. [3] explored the applicability of the effective notch stress approach to fatigue assessment of cruciform joints, considering fatigue crack initiation points, stress distributions and fatigue strengths. Aygül et al. [4] evaluated the application of the structural hot spot stress approach and the effective notch stress approach to a welded joint with cutout holes in orthotropic bridge decks. The calculated results revealed that the structural hot spot stresses obtained from the shell element models were unrealistically high when the welds were omitted. Mustafa discussed weld end modeling of cope-hole details in Ref. [5]. So far, a large number of fatigue experiments for these welded details have been conducted under repeated cyclic loads, and a set of fatigue life curves were produced or fitted according to fatigue experiment result. Besides, these curves have now been included in current relevant fatigue specifications [6, 7], such as Eurocode3 and IIW (International Institute of Welding) documents. However, in view of steel material, welding technology and stress pattern of new girder structure details

✉ Renda Zhao  
rendazhao@163.com

<sup>1</sup> School of Civil Engineering, Southwest Jiaotong University, Chengdu 610031, China

different from similar welded details in current relevant fatigue specifications, anti-fatigue design codes of similar welded details cannot be directly used for new girder structural details. So Liao et al. [8–11] carried out fatigue experimental research on this welded constructional details (called welded detail I in the following). Based on the experimental results and the least squares method, the S–N curve of this welded detail was fitted. Through the analysis of fatigue performance experiments of welded detail I, the fatigue performance of this welded detail was relatively poor. In order to ameliorate and improve its fatigue performance, this paper proposed an optimization measure of plate filled in cope hole, and fatigue experiments and the finite element method were used to study the improvement effect of optimized welded detail.

In Refs. [12–15], the influence factors of stress concentration for the load and non-load carrying cruciform welded joints, such as toe angle, weld size, weld toe radius, assembly misalignment, mesh size and weld gap, were analyzed. However, works dealing with the fatigue performance of optimized welded detail are scarce. In this work, in order to improve its fatigue performance, three specimens with the same details as those in Refs. [12–15] were subjected to nominal stress with the amplitudes of 99, 90 and 63 MPa, respectively, and tested for fatigue failure. Finally, the finite element method was used to discuss these influence factors of the stress concentration effects.

## 2 Fatigue experiment of optimized welded detail

### 2.1 Geometry dimensions

Welded detail I uses the cruciform section with cope holes, and its web is integral. The overall geometry and the cross-sectional form of optimized welded detail are identical with welded detail I given in Ref. [8], except that a semicircular plate with a thickness of 10 mm is filled in the cope hole and its radius is slightly smaller than that of the cope hole. The semicircular plate is aligned at a surface of the web, both of which are joined by groove welding, as shown in Fig. 1. The thickness of flange and web for the optimized welded detail is 16 mm, and fillet weld size is 8 mm. In addition, the cope holes of optimized welded detail are filled with semicircular plate whose thickness is 10 mm. Figure 1 shows the size and structure of optimized welded detail.

### 2.2 Fatigue experiment loading

Three specimens of optimized welded detail loaded with different stress amplitudes were designed and manufactured by common steel plate with the grade of Q345C.

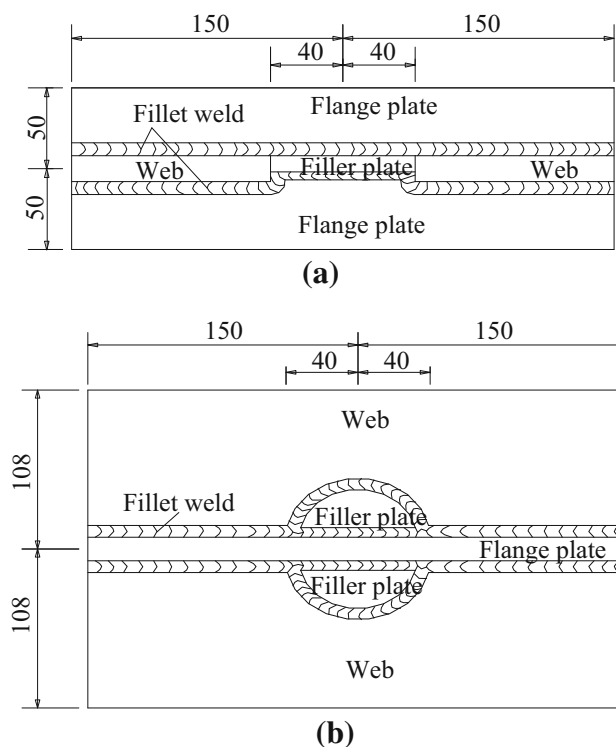


**Fig. 1** Geometric dimensions of optimized welded detail (unit: mm). **a** Flange dimension, **b** web dimension

Nominal stresses of 99, 90 and 63 MPa were applied to the end of every specimen, respectively. These three kinds of nominal stress applied to the specimens were mainly determined according to fatigue experiment of similar welded details and S–N curve in the fatigue specification. This load was sinusoidal with stress ratio 0.1, and the loading frequency was 3 Hz. Besides, load was carried out by fatigue testing machine with the load capacity of 500 and 1000 kN. The loading experimental setup is shown in Fig. 2, and fatigue failure is illustrated in Fig. 3. According to the fatigue experiment results, the fatigue life of the



**Fig. 2** Loading setup



**Fig. 3** Fatigue fracture of the specimen

specimens of optimized welded detail was 736,000, 1,044,200 and 1,920,300 times, respectively.

### 3 Finite element simulation and analysis

#### 3.1 Finite element modeling

In order to reduce the calculation time, the section model for optimized welded detail was established and the model appropriately extended along the length direction of the region of interest to exclude end loading and boundary constraint effect on local stress distribution. In the modeling process, the fillet weld was simplified as a triangular cross section, and all parts were simulated by solid element SOLID45 in ANSYS [16]. The finite element fictional results at zones with stress concentration are eliminated by comparing and analyzing the local stress concentration coefficients of the welding parts with different grid sizes. On the basis of the above comparison results, considering the efficiency and accuracy of the analysis, the unit size is determined finally. The hexagonal element was used for meshing, and the cell size was 0.5 cm. Two symmetrical

nodes were generated at a distance of 20 cm from the end of the model. Two rigid regions were established between nodes and near end surface of this welded detail. Concentrated load of 345 kN was applied at one node, and the fixed constraint was applied at the other node. The established finite element model is shown in Fig. 4.

In the following finite element analysis, elastic modulus and Poisson's ratio of the weld were assumed to be the same as those of the flange and the web, and a linear elastic model is used. Modulus of elasticity and Poisson's ratio and weld toe angle are taken to be 207 GPa, 0.3 and 45°, respectively. Yield strength of steel is 345 MPa. In addition, the transition arc between weld toe and plate was ignored in the modeling.

#### 3.2 Finite element results

Optimized welded detail is subjected to uniaxial tensile load, and the difference between the first principal stress and the maximum longitudinal stress is small for this detail. Therefore, the stress concentration factor only calculated by the maximum longitudinal stress is sufficient to reflect the local stress concentration of this detail. In order to compare the stress distribution and SCC of each component of optimized welded detail and welded detail I, the results calculated by finite element models of these welded details are summarized in Table 1 and Fig. 5. In Table 1,  $\sigma_{1\max}$ ,  $\sigma_{2\max}$  and  $\sigma_{3\max}$  represent the maximum longitudinal stress of web, flange and weld, respectively. And  $\sigma$  means the nominal stress (70 MPa) of a certain distance from core research region. In addition,  $K_1$ ,  $K_2$  and  $K_3$  represent the stress concentration coefficients (SCCs) of the web, flange and weld, respectively.

$$K_1 = \sigma_{1\max} / \sigma, \quad (1)$$

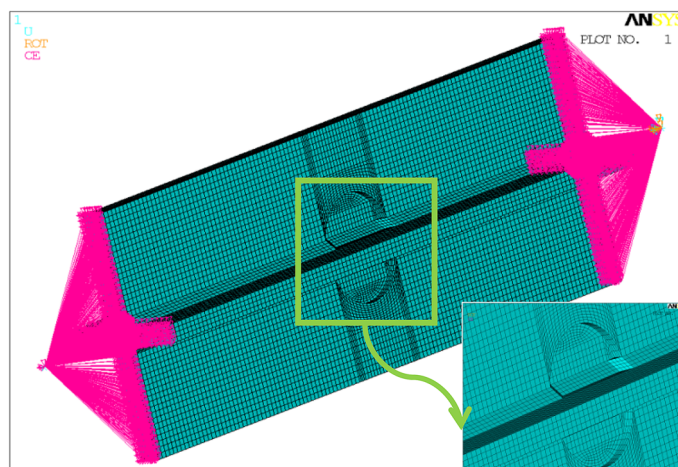


**Fig. 4** A finite element model and meshing

**Table 1** Finite element calculation results of welded details

Detail code	$\sigma_{1\max}$	$K_1$	$\sigma_{2\max}$	$K_2$	$\sigma_{3\max}$	$K_3$
Welded detail I	197	2.81	161	2.30	169	2.41
Optimized welded detail	138	1.97	97.8	1.40	124	1.77

$$K_2 = \sigma_{2\max}/\sigma, \quad (2)$$

$$K_3 = \sigma_{3\max}/\sigma. \quad (3)$$

As shown in Table 1, the SCCs of web, flange and weld for welded detail I are higher than those of optimized welded detail. The component with the maximum longitudinal stress among of welded detail I and optimized welded detail parts is web and weld, respectively. In addition, the maximum longitudinal stress of weld for each welded detail is higher than that of flange.

#### 4 Parametric studies

In the manufacturing and assembling process of steel bridges, there may be abrupt change in the cross-sectional geometry near the weld toe, plate misalignment, initial

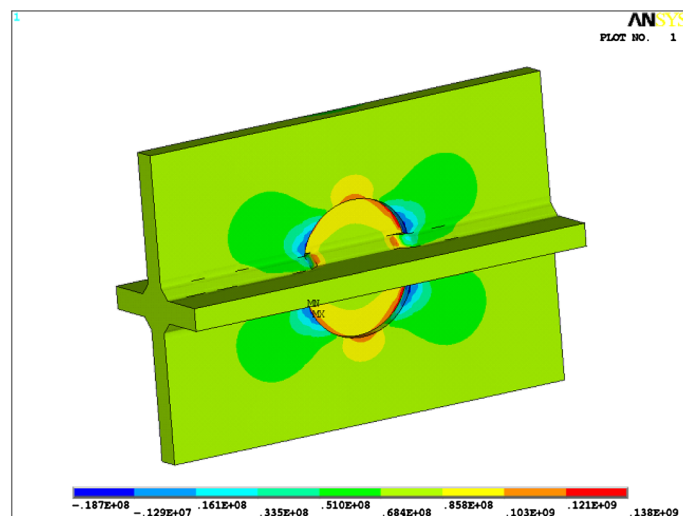
geometric imperfections, the plate gap and weld penetration. Therefore, because of the local stress concentration phenomenon, the fatigue crack is easy to occur and expand at the weld toe or root. Based on the results of stress analysis, an attempt was made to construct simple relationships among the stress concentration and above parameters.

In this part, the dimensions of optimized welded detail in the parametric studies are shown in Table 2.

##### 4.1 Plate thickness

In order to study the influence of flange and web thickness of optimized welded detail on the SCC, the flange and web thicknesses will be changed, respectively, between 12 and 20 mm (considering the case of the medium plate). Figures 6–14 illustrate the SCC variation affected by plate thickness, weld size, cope-hole radius, filler plate thickness, plate gap with, weld penetration parameters and initial geometric imperfection, respectively.

With the increase in flange thickness, the SCC of web for optimized welded detail only changes 1.4%. When flange thickness changes from 12 to 20 mm, the SCC of the flange decreases gradually and its variation is within 5.5%.

**Fig. 5** Finite element results of optimized welded detail**Table 2** Dimension of welded details used in parametric studies (in mm)

Flange plate thickness	12.00	13.00	14.00	15.00	16.00	17.00	18.00	19.00	20.00
Web thickness	12.00	13.00	14.00	15.00	16.00	17.00	18.00	19.00	20.00
Weld size	6.00	6.50	7.00	7.50	8.00	8.50	9.00	9.50	10.00
Cope-hole thickness	24.00	28.00	32.00	36.00	40.00	44.00	48.00	52.00	56.00
Filler plate thickness	8.00	8.50	9.00	9.50	10.00	10.50	11.00	11.50	12.00
Weld penetration parameters	0.25	0.50	0.75	1.00	1.25	1.50	1.75	2.00	2.25
Initial geometric imperfection	5.00	6.00	7.00	8.00	9.00	10.00	11.00	12.00	13.00

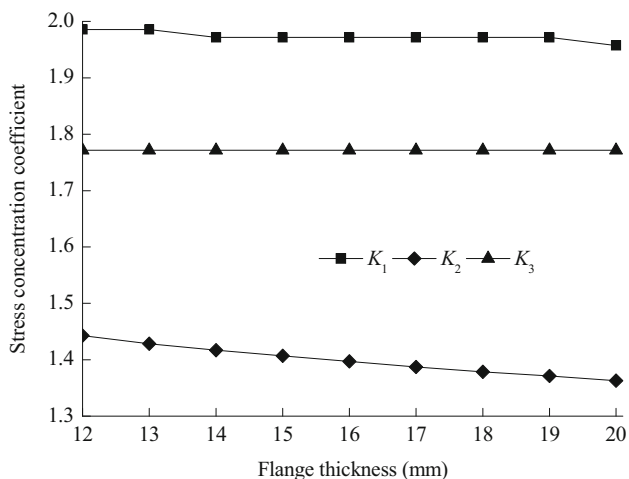


Fig. 6 Relationship between SCC and flange thickness

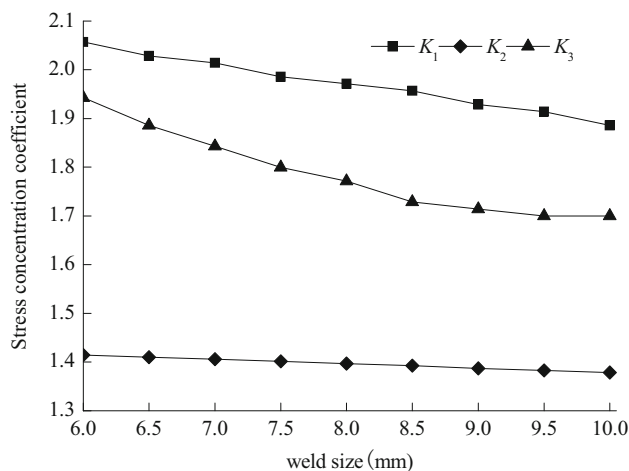


Fig. 8 Relationship between SCC and weld size

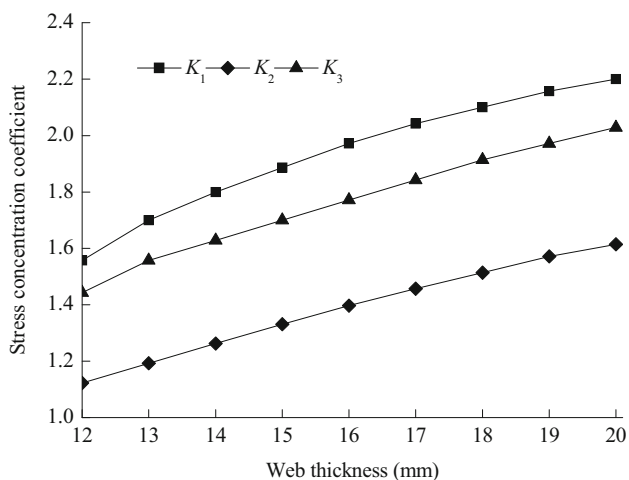


Fig. 7 Relationship between SCC and web thickness

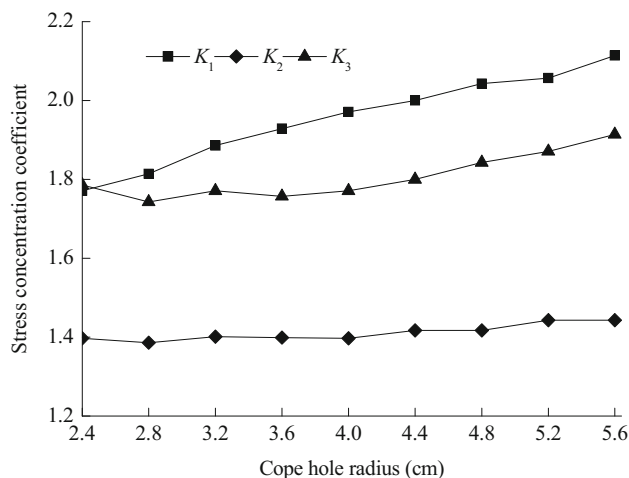


Fig. 9 Relationship between SCC and the cope-hole radius

However, the SCC of weld is hardly affected by flange thickness. Therefore, as shown in Fig. 6, the SCC of optimized welded detail for each component is less affected by the flange thickness.

From Fig. 7, the SCCs of the web, flange and weld of the optimized welded detail increase with the web thickness and the relationship is approximately linear. When web thickness changes from 12 mm to 20 mm, the variation of the SCC of each component is 41.3, 43.8 and 40.6%, respectively. In summary, the SCCs of optimized welded detail are significantly affected by web thickness.

#### 4.2 Weld size

The weld is taken as an important force transmission component that connects flange and web for optimized welded detail. In order to investigate the influence of the

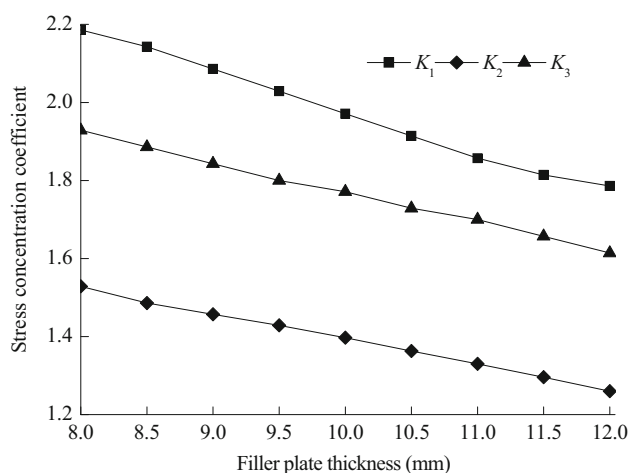
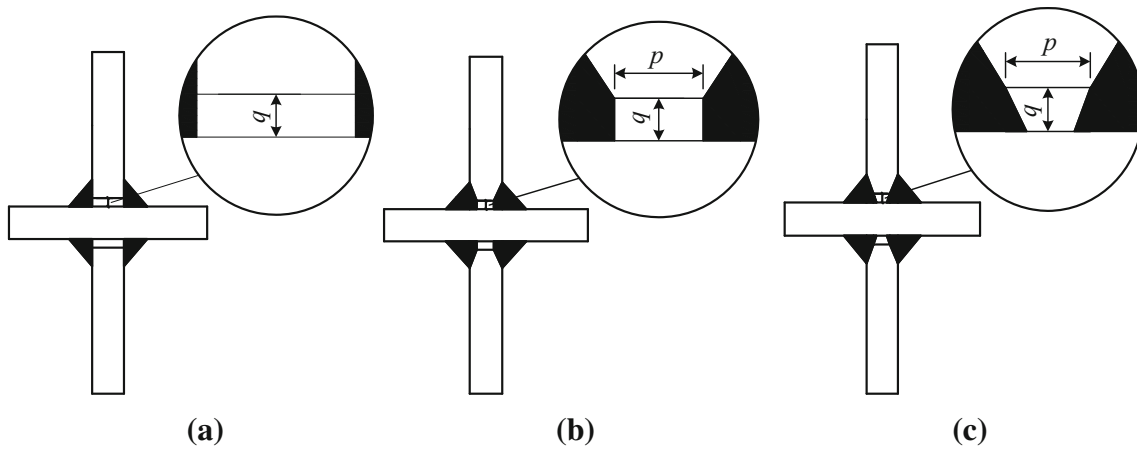
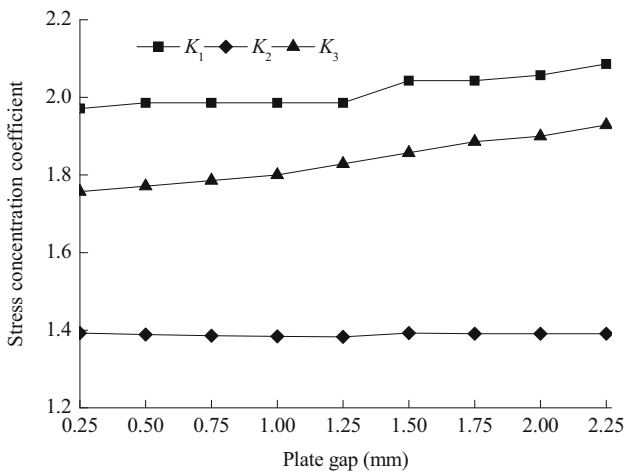


Fig. 10 Relationship between SCCs and the filler plate thickness



**Fig. 11** Schematic diagram of plate gap parameters. **a** Gap width, **b** gap length for Type I, **c** gap length for Type 2



**Fig. 12** Relationship between the SCC and plate gap width

weld size, the weld toe size changes in the range of 6–10 mm and the calculated results by the finite element models are shown in Fig. 8.

As shown in Fig. 8, the SCC of each component decrease with the increase in weld size. When weld size changes from 6.0 to 10.0 mm, the variation of the SCC for the web, flange and weld is 8.3, 2.5 and 12.5%, respectively. Therefore, the SCCs of web and the weld are more affected by the weld size.

### 4.3 Cope-hole radius

Although a semicircular plate with a certain thickness is filled in the cope hole of optimized welded detail, the cope-hole radius has some influence on SCC of each component. In order to investigate the influence of cope-hole radius, the cope-hole radius is changed between 2.4 and 5.6 cm and the results are shown in Fig. 9.

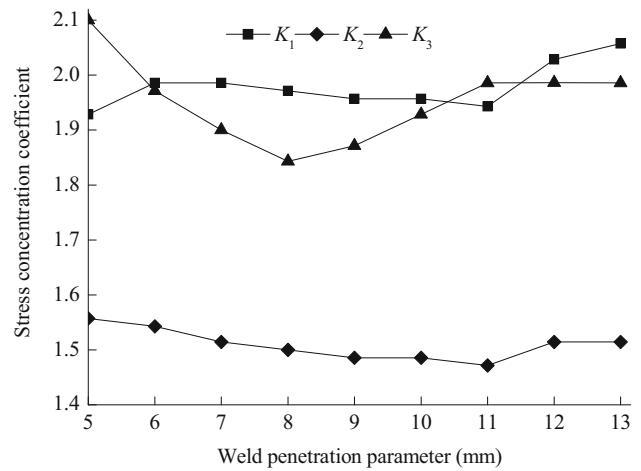


**Fig. 13** Relationship between the SCC and weld penetration parameter

From Fig. 9, with the increase in the cope-hole radius, there is nearly linear increase in SCC of each component. When cope-hole radius changes from 2.4 to 5.6 mm, the SCC variation of web, flange and weld is 19.4, 3.3 and 7.2%, respectively. As a result, the SCCs of web and weld are more affected by the cope-hole radius than that of the flange.

### 4.4 Filler plate thickness

Optimized welded detail has cope holes which are filled by a semicircular plate with a certain thickness. Here, the filler plate thickness changes between 8 and 12 mm and the results of finite element analysis are shown in Fig. 10.

Note that the SCC of each component of optimized welded detail decreases gradually with the increase in the filler plate thickness and their relationship is approximately linear. When the filler plate thickness changes from 8.0 to

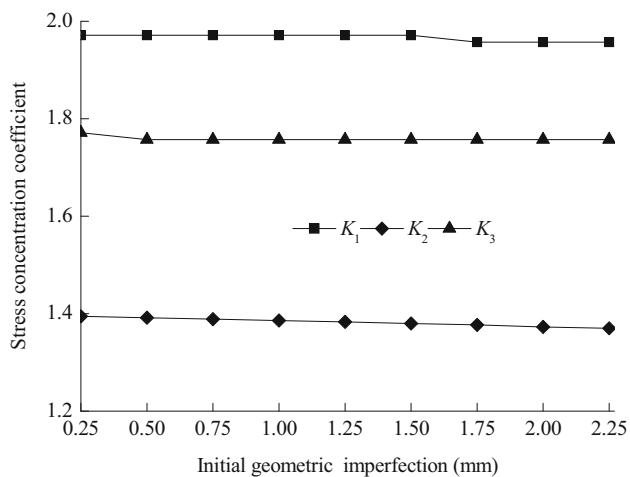


**Fig. 14** Relationship between the SCC and initial geometric imperfection

12.0 mm, the SCC variation of web, flange and weld is 18.3, 17.6 and 16.3%, respectively. Therefore, the SCC of each component is obviously affected by the change in the filler plate thickness.

#### 4.5 Plate gap width

As shown in Fig. 10, welded details in the manufacturing process have a certain assembly gap (or plate space) between flange and web, and the main parameters of the assembly gap are the gap width  $q$  and the gap length  $p$ . Large assembly gap is easy to cause large shrinkage deformation of the weld and the waste of flux material [17]. The test results of Ref. [18] show that the gap width of cruciform welded joints is 0.5 mm. When studying the influence of the gap width of the load and non-load cruciform welded joints, it is assumed that the gap width is 0–2 mm [17]. Here we assume that the variation range of the gap width is 0.25–2.25 mm. Figure 12 presents the relationship between the SCC and plate gap width.

It can be seen from Fig. 12 that the SCCs of the web and weld increase with the plate gap width and the amplitude is 1.5, 5.8 and 9.8%, respectively. However, the SCC of flange is hardly affected by the plate gap width. Therefore, the plate gap width has large effect on the SCC of the weld, while the SCCs of the flange and web are less affected by the plate gap width.

#### 4.6 Weld penetration parameters

The weld penetration parameter is defined as

$$L = (H - p)/2, \quad (4)$$

where  $H$  is the web thickness and the range of  $L$  is 5–13 mm. The simplified analysis model of the penetration

weld illustrated in Fig. 11b was built, and the calculated results are shown in Fig. 13.

As can be seen from Fig. 13, when the weld penetration parameter increase from 6 to 13 mm, the SCC of each component firstly reduces and then increases, and the variation of SCC of web, flange and weld is 6.7, 5.5 and 12.2%, respectively. As a result, it is possible to conclude that weld penetration parameter is a main factor controlling severity of SCC for weld.

#### 4.7 Initial geometric imperfection

In the process of welding and manufacturing, fatigue specimens may produce certain initial geometric imperfections such as initial bending, and the SCC of each component will be influenced. Initial geometric imperfection of optimized welded detail was considered by introducing different percentages of characteristic values of the first-order buckling mode shape in this paper [19]. The variation range of initial defection is 0.25–2.25 mm. The calculated results are shown in Fig. 14.

As shown in Fig. 14, the SCC of each component for the optimized welded details is less affected by initial geometric imperfection and the variation amplitude is less than 2.9%.

### 5 Conclusions

The fatigue life of optimized welded detail was tested by fatigue experiment, and the SCC of each component was investigated by finite element method. The following conclusions can be reached:

1. The fatigue life of three specimens of optimized welded detail is 736,000, 1,044,200 and 1,920,300 times, respectively. Under the same nominal stress amplitude, the fatigue performance of the specimens of the optimized welded detail is better than that of welded detail I, which indicates that optimized welded detail is superior.
2. The SCC of each component of optimized welded detail is less affected by web thickness, filler plate thickness and initial geometric imperfections, but the influence of cope-hole radius is very significant.
3. The SCC of the weld for optimized welded detail is significantly affected by the weld size, gap width and gap length, but those of other parts for optimized welded detail are less affected.

**Acknowledgements** This work is supported by the National Natural Science Foundation of China (51308467 and 51378431) and China railway corporation research and development of science and

technology key project (2013G001-A-2). The support is gratefully acknowledged.

**Open Access** This article is distributed under the terms of the Creative Commons Attribution 4.0 International License (<http://creativecommons.org/licenses/by/4.0/>), which permits unrestricted use, distribution, and reproduction in any medium, provided you give appropriate credit to the original author(s) and the source, provide a link to the Creative Commons license, and indicate if changes were made.

## References

- Chiew SP, Lie ST, Lee CK et al (2004) Fatigue performance of cracked tubular T joints under combined loads. I: experimental. *J Struct Eng* 130(4):562–571
- Miki C, Tateishi K (1997) Fatigue strength of cope hole details in steel bridges. *Int J Fatigue* 19(6):445–455
- Park W, Miki C (2008) Fatigue assessment of large-size welded joints based on the effective notch stress approach. *Int J Fatigue* 30(9):1556–1568
- Aygül M, Al-Emrani M, Urushadze S (2012) Modelling and fatigue life assessment of orthotropic bridge deck details using FEM. *Int J Fatigue* 40(7):129–142
- Mustafa A (2012) Fatigue analysis of welded structures using the finite element method. Dissertation, Chalmers University of Technology
- European Committee for Standardization. Eurocode3 (2005) Design of steel structures, Part 1-9: Fatigue (EN1993-1-9:2005). London, Britain
- Recommendations For Fatigue Design Of Welded Joints And Components (2008) IIW document IIW-1823-07ex XIII-2151r4-07/XV-1254r4-07. Paris, France
- Xiao ZG, Yamada K (2004) A method of determining geometric stress for fatigue strength evaluation of steel welded joints. *Int J Fatigue* 26(12):1277–1293
- Li DC, Liu HL (1992) The influence of weld toe angle and leg length on stress concentration factor of cross-shaped joint. *J Mech Eng* 28(1):49–52 (in Chinese)
- Yu QM, Song SY, Yin Q et al (1995) The effects of the position deviation on the fatigue life and structural strength of the cross joint. *Jiangsu Ship* (3):39–46. (in Chinese)
- Zhang Y, Huang XP, Cui WC et al (2004) Finite element analysis on stress concentration at weld toe of butt-welded joint. *J Ship Mech* 8(5):91–99 (in Chinese)
- Liao P, Wei X, Xiao L et al (2016) Experimental research on the girder's new detail fatigue performance of Hutong railway Yangtze river bridge. *Chin Civil Eng J* 49(6):76–83 (in Chinese)
- Liao P, Xiao L, Wei X et al (2016) Fatigue life prediction and parameter analysis of girder new detail. *J Southwest Jiaotong Univ* 51(4):639–644 (in Chinese)
- Liao P, Wei X, Xiao L et al (2017) Optimization and experimental study of fatigue performance of welded details with cope holes. *Bridge Constr* 47(2):37–41 (in Chinese)
- Liao P (2014) The fatigue performance analysis on the welded detail of cope hole of the ventral rod of steel truss bridge. Dissertation, Southwest Jiaotong University. (in Chinese)
- ANSYS (2009) Release 12.0 documentation for ANSYS. ANSYS, Inc., Pittsburgh
- Wu Q (2009) Fatigue analysis of welded joints and fatigue life estimation of multi-axis high cycle based on structural stress. Dissertation, Tongji University. (in Chinese)
- Wu B (2003) Fatigue failure assessment method for stainless steel welded joints. Dissertation, Tianjin University. (in Chinese)
- Wang XM (2007) ANSYS engineering structure numerical analysis. China communication press, Beijing. (in Chinese)